PHYSICAL REVIEW D **95,** 094506 (2017)

New approach to canonical partition functions computation in $N_f = 2$ lattice QCD at finite baryon density

V. G. Bornyakov

Institute for High Energy Physics NRC Kurchatov Institute, 142281 Protvino, Russia, Institute of Theoretical and Experimental Physics NRC Kurchatov Institute, 117218 Moscow, Russia, and School of Biomedicine, Far Eastern Federal University, 690950 Vladivostok, Russia

D. L. Boyda and V. A. Goy

School of Natural Sciences, Far Eastern Federal University, 690950 Vladivostok, Russia, School of Biomedicine, Far Eastern Federal University, 690950 Vladivostok, Russia, and Institute of Theoretical and Experimental Physics NRC Kurchatov Institute, 117218 Moscow, Russia

A. V. Molochkov

School of Biomedicine, Far Eastern Federal University, 690950 Vladivostok, Russia, and Institute of Theoretical and Experimental Physics NRC Kurchatov Institute, 117218 Moscow, Russia

Atsushi Nakamura

School of Biomedicine, Far Eastern Federal University, 690950 Vladivostok, Russia, Research Center for Nuclear Physics (RCNP), Osaka University, Ibaraki, Osaka 567-0047, Japan, and Theoretical Research Division, Nishina Center, RIKEN, Wako 351-0198, Japan

A. A. Nikolaev

School of Biomedicine, Far Eastern Federal University, 690950 Vladivostok, Russia, and Institute of Theoretical and Experimental Physics NRC Kurchatov Institute, 117259 Moscow, Russia

V. I. Zakharov

Institute of Theoretical and Experimental Physics NRC Kurchatov Institute, 117259 Moscow, Russia School of Biomedicine, Far Eastern Federal University, 690950 Vladivostok, Russia, and Moscow Institute of Physics and Technology, Dolgoprudny, Moscow Region, 141700 Russia

(Received 18 November 2016; published 16 May 2017)

We propose and test a new approach to computation of canonical partition functions in lattice QCD at finite density. We suggest a few steps procedure. We first compute numerically the quark number density for imaginary chemical potential $i\mu_{qI}$. Then we restore the grand canonical partition function for imaginary chemical potential using the fitting procedure for the quark number density. Finally we compute the canonical partition functions using high precision numerical Fourier transformation. Additionally we compute the canonical partition functions using the known method of the hopping parameter expansion and compare results obtained by two methods in the deconfining as well as in the confining phases. The agreement between two methods indicates the validity of the new method. Our numerical results are obtained in two flavor lattice QCD with clover improved Wilson fermions.

DOI: 10.1103/PhysRevD.95.094506

I. INTRODUCTION

One of the most important research targets in high energy and nuclear physics is to reveal the hadronic matter phase structure at finite temperature and density. Experiments at most important modern accelerators RHIC (BNL) [1], LHC (CERN) [2] and future experiments FAIR (GSI) and NICA (JINR) are devoted to such studies. Towards this goal, experimental, observational and theoretical efforts have been made. The lattice QCD numerical simulations have a mission to provide data from the first principle calculations. Indeed, at finite temperature with zero chemical potential, the phase structure was satisfactorily investigated. But it is very difficult to study lattice QCD at finite density because of the infamous "sign problem": The fermionic determinant at nonzero baryon chemical potential μ_B, $\det\Delta(\mu_B)$, is in general not real. This makes impossible to apply standard Monte Carlo techniques to computations with the partition function

$$Z_{GC}(\mu_q, T, V) = \int \mathcal{D}U(\det\Delta(\mu_q))^{N_f} e^{-S_G}, \qquad (1)$$

where S_G is a gauge field action, $\mu_q = \mu_B/3$ is quark chemical potential, $T = 1/(aN_t)$ is temperature,

$V = (aN_s)^3$ is volume, a is lattice spacing, N_t, N_s is number of lattice sites in time and space directions. There have been many trials (see e.g. reviews [3–5]) and yet it is still very hard to get reliable results at $\mu_B/T > 1$, see Ref. [6].

In this paper, we consider two approaches: canonical approach and analytical continuation from imaginary chemical potential. Our motivation is to develop a method of computations in finite density lattice QCD applicable at large μ_B/T to compute theoretically and experimentally interesting physical quantities such as number density, its susceptibility and higher cumulants as well as pressure and energy density. The canonical approach was studied in a number of papers [7–14]. The analytical continuation was also found a useful tool to compute the listed above physical quantities [5] or the curvature in the transition temperature as a function of the chemical potential [5].

We suggest a new method to compute canonical partition functions $Z_C(n, T, V)$ including large values of n where n is a net number of quarks and antiquarks. We will show that results for $Z_C(n, T, V)$ obtained with the new method are in good agreement with results obtained with the known method of hopping parameter expansion (HPE). Then we will argue that the analytical continuation might work beyond the validity of the Taylor expansion method.

The new method is based on simulations at the imaginary chemical potential. We explain the details of the new method in the next section. In Sec. III details of numerical simulations including explanation of main features of the hopping parameter expansion are presented. Numerical results for a few values of temperature in both confinement and deconfinement phases and comparison with the hopping parameter expansion are presented in Sec. IV. Finally, we formulate our conclusions in Sec. V.

II. NEW APPROACH TO COMPUTATION OF CANONICAL PARTITION FUNCTION

The canonical approach is based on the following relations. First, this is a relation between grand canonical partition function $Z_{GC}(\mu_q, T, V)$ and the canonical one $Z_C(n, T, V)$,

$$Z_{GC}(\mu_q, T, V) = \sum_{n=-\infty}^{\infty} Z_C(n, T, V)\xi^n, \tag{2}$$

where $\xi = e^{\mu_q/T}$ is the fugacity and Eq. (2) is called fugacity expansion. The inverse of this equation can be presented in the following form [15]:

$$Z_C(n, T, V) = \int_0^{2\pi} \frac{d\theta}{2\pi} e^{-in\theta} Z_{GC}(\theta, T, V). \tag{3}$$

In the right-hand side of Eq. (3) we see the grand canonical partition function $Z_{GC}(\theta, T, V)$ for imaginary chemical potential $\mu_q = i\mu_{qI} \equiv iT\theta$. It is known that standard Monte Carlo simulations are possible for this partition function since the fermionic determinant is real for imaginary μ_q.

The QCD partition function Z_{GC} is a periodic function of θ: $Z_{GC}(\theta) = Z_{GC}(\theta + 2\pi/3)$. As a consequence of this periodicity the canonical partition functions $Z_C(n, T, V)$ are nonzero only for $n = 3k$. This symmetry is called Roberge-Weiss symmetry [16]. QCD possesses a rich phase structure at nonzero θ, which depends on the number of flavors N_f and the quark mass m. This phase structure is shown in Fig. 1. T_c is the confinement/deconfinement crossover point at zero chemical potential. The line $(T \geq T_{\mathrm{RW}}, \mu_I/T = \pi/3)$ indicates the first order phase transition. On the curve between T_c and T_{RW}, the transition is expected to change from the crossover to the first order for small and large quark masses, see e.g. [17].

Quark number density n_q for N_f degenerate quark flavors is defined by the following equation:

$$\frac{n_q}{T^3} = \frac{1}{VT^2}\frac{\partial}{\partial\mu_q}\ln Z_{GC} = \frac{N_f N_t^3}{N_s^3 Z_{GC}} \int \mathcal{D}U e^{-S_G} (\det \Delta(\mu_q))^{N_f} \mathrm{tr}\left[\Delta^{-1}\frac{\partial\Delta}{\partial\mu_q/T}\right]. \tag{4}$$

It can be computed numerically for imaginary chemical potential. Note that for the imaginary chemical potential n_q is also purely imaginary: $n_q = in_{qI}$.

From Eqs. (2) and (5) it follows that densities n_q and n_{qI} are related to $Z_C(n, T, V)$ [below we will use the notation Z_n for the ratio $Z_C(n, T, V)/Z_C(0, T, V)$] by equations

$$n_q/T^3 = \mathcal{N}\frac{2\sum_{n>0} nZ_n \sinh(n\theta)}{1 + 2\sum_{n>0} Z_n \cosh(n\theta)}, \tag{5}$$

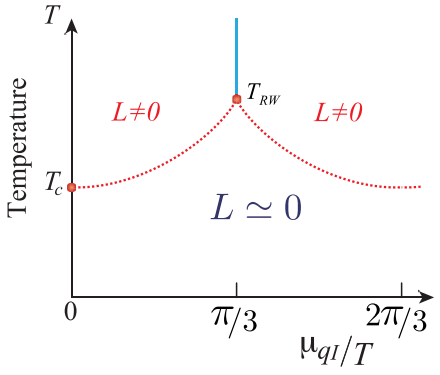

FIG. 1. Schematical figure of Roberge-Weiss phase structure in the pure imaginary chemical potential regions. T_c is the confinement/deconfinement crossover point at zero chemical potential, L is the Polyakov loop. The vertical line $(T \geq T_{\mathrm{RW}}, \mu_I/T = \pi/3)$ shows the first order phase transition. The dashed line is a crossover which can change to the first order phase transition for large or small quark masses.

$$n_{qI}/T^3 = \mathcal{N}\frac{2\sum_{n>0} nZ_n \sin(n\theta)}{1+2\sum_{n>0} Z_n \cos(n\theta)}, \quad (6)$$

where $\mathcal{N}$ is a normalization constant, $\mathcal{N} = \frac{N_t^3}{N_s^3}$. Our suggestion is to compute Z_n using Eq. (6).

One way to do this is to fit numerical data for n_{qI} to this functional form with a finite number of terms in both numerator and denominator with Z_n treated as a fitting parameters. We tried this method and found that it is difficult to obtain reliable values of Z_n.

We found more successful the following approach. One can compute $Z_{GC}(\theta, T, V)$ using numerical data for n_{qI}/T^3 via numerical integration over the imaginary chemical potential:

$$L_Z(\theta) \equiv \log\frac{Z_{GC}(\theta,T,V)}{Z_{GC}(0,T,V)} = -V\int_0^\theta d\tilde{\theta} n_{qI}(\tilde{\theta}), \quad (7)$$

where we omitted T and V from the grand canonical partition function notation. Then Z_n can be computed as

$$Z_n = \frac{\int_0^{2\pi}\frac{d\theta}{2\pi} e^{-in\theta} e^{L_Z(\theta)}}{\int_0^{2\pi}\frac{d\theta}{2\pi} e^{L_Z(\theta)}}. \quad (8)$$

In the present work we use a modified version of this approach. Instead of numerical integration in (7) we fitted n_{qI}/T^3 to theoretically motivated functions of μ_{qI}.

It is known that the density of noninteracting quark gas is described by

$$n_q/T^3 = N_f\left(2\frac{\mu_q}{T} + \frac{2}{\pi^2}\left(\frac{\mu_q}{T}\right)^3\right). \quad (9)$$

This allows one to assume that in the deconfinement phase the density can be fitted to the polynomial function. Indeed, it was shown in Ref. [18], where the same lattice action was simulated, that such a function describes the number density in the deconfinement phase quite well. This observation was also confirmed in Ref. [19] where $N_f = 2+1$ lattice QCD with physical quark masses was studied. We thus fit the data for n_{qI} to an odd power polynomial of θ,

$$n_{qI}(\theta)/T^3 = \sum_{n=1}^{n_{\max}} a_{2n-1}\theta^{2n-1}, \quad (10)$$

in the deconfining phase.

It is well known that in the confining phase (below T_c) the hadron resonance gas model provides a good description of the chemical potential dependence of thermodynamic observables [20]. Thus it is reasonable to fit the density to a Fourier expansion,

$$n_{qI}(\theta)/T^3 = \sum_{n=1}^{n_{\max}} f_{3n}\sin(3n\theta). \quad (11)$$

Again this type of fit was used in Ref. [18] and a conclusion was made that it works well.

Using these fits and Eqs. (7) and (8), we obtained very promising results for the canonical partition functions Z_n as will be shown in Sec. IV.

III. SIMULATION SETTINGS

To demonstrate our method we make simulations of the lattice QCD with $N_f = 2$ clover improved Wilson quarks and Iwasaki improved gauge field action:

$$S = S_g + S_q, \quad (12)$$

$$S_g = -\beta\sum_{x,\mu\nu}(c_0 W^{1\times1}_{\mu\nu}(x) + c_1 W^{1\times2}_{\mu,\nu}(x)), \quad (13)$$

$$S_q = \sum_{f=u,d}\sum_{x,y}\bar{\psi}^f_x \Delta_{x,y}\psi^f_y, \quad (14)$$

where $\beta = 6/g^2$, $c_1 = -0.331$, $c_0 = 1\text{–}8c_1$,

$$\begin{aligned}\Delta_{x,y} = \delta_{xy} &- \kappa\sum_{i=1}^{3}\{(1-\gamma_i)U_{x,i}\delta_{x+\hat{i},y} + (1+\gamma_i)U^\dagger_{y,i}\delta_{x,y+\hat{i}}\} \\ &- \kappa\{e^{a\mu_q}(1-\gamma_4)U_{x,4}\delta_{x+\hat{4},y} \\ &+ e^{-a\mu_q}(1+\gamma_4)U^\dagger_{y,4}\delta_{x,y+\hat{4}}\} \\ &- \delta_{xy}c_{\rm SW}\kappa\sum_{\mu<\nu}\sigma_{\mu\nu}P_{\mu\nu}, \end{aligned} \quad (15)$$

$P_{\mu\nu}$ is the clover definition of the lattice field strength tensor, and $c_{\rm SW} = (W^{1\times1})^{-3/4} = (1-0.8412\beta^{-1})^{-3/4}$ is the Sheikholeslami-Wohlert coefficient.

We simulate $16^3\times4$ lattices at temperatures $T/T_c =$ 1.35, 1.20 and 1.08 in the deconfinement phase and 0.99,0.93,0.84 in the confinement phase along the line of constant physics with $m_\pi/m_\rho = 0.8$. All parameters of the action, including $c_{\rm SW}$ value, were borrowed from the WHOT-QCD collaboration paper [21]. We compute the number density on samples of $N_{\rm conf}$ configurations with $N_{\rm conf} = 1800$, using every tenth trajectory produced with the hybrid Monte Carlo algorithm.

We employ the hopping parameter expansion to compute Z_n and compare with Z_n values obtained with our new method. Below we describe the hopping parameter expansion. The hopping parameter expansion was invented to estimate the dynamical quark loop effects [22,23], and since then, this method has been accepted as an effective tool for the lattice QCD with heavy quarks [24–27]. In Ref. [28], the fugacity expansion of the fermion determinant is obtained for the Wilson fermions and the canonical

partition functions, Z_n are evaluated. This means that $Z_{GC}(\mu_q, T, V)$ can be computed in the lattice QCD for finite μ_q via Eq. (2). Therefore, the question is whether we can obtain reliable Z_n or not in numerical simulations. The Wilson Dirac operator from (1) may be written in the form

$$\Delta = I - \kappa Q, \tag{16}$$

both in the case of standard and clover improved Wilson fermions. Then one can rewrite the fermionic determinant in the following way [14]:

$$\det \Delta = \exp[\mathrm{Tr}\ln(I - \kappa Q)] = \exp\left[-\sum_{n=1}^{\infty}\frac{\kappa^n}{n}\mathrm{Tr}Q^n\right]. \tag{17}$$

The chemical potential is introduced in the Dirac operator in the form of $e^{\pm a\mu_q}$ multipliers in the temporal direction links $U_{x,4}$. The expansion in (17) is in fact expansion over the closed paths on the lattice, and thus (17) can be rewritten as

$$\det \Delta = \exp\left[\sum_{n=-\infty}^{\infty} W_n \xi^n\right], \tag{18}$$

where n is number of windings in the temporal direction, and W_n are complex coefficients which are called winding numbers. They satisfy the property $W_{-n} = W_n^*$. In the case of the imaginary chemical potential the expansion (18) will become

$$\det \Delta = e^{W_0} e^{2\sum_{n=1}^{\infty}(\mathrm{Re}[W_n]\cos(n\theta) - \mathrm{Im}[W_n]\sin(n\theta))}. \tag{19}$$

It is important to note that the hopping parameter expansion (17) and the winding number expansion (18) converge properly only for the heavy quark masses [14]. Our simulations were performed for the quark masses from this range. The hopping parameter expansion is used to compute the winding numbers W_n introduced in Eq. (18). We cut the summation in Eqs. (17) and (18). The effects of these cuts are discussed in detail in Ref. [29], see in particular Fig. 2 of Ref. [29]. In particular we found that W_n do not change within statistical error bars for $|n| \leq 15$ if we use $n_{\mathrm{hpe}} \geq 300$ terms in the hopping parameter expansion Eq. (17). Furthermore, we found that using $n_{\mathrm{wne}} = 15$ terms in Eq. (18) is enough to obtain Z_n for $n \leq 150$ in the deconfinement phase at $T/T_c = 1.35$ and Z_n for $n \leq 30$ in the confinement phase at $T/T_c = 0.93$ (in the confinement phase we encounter a substantial overlap problem).

We compute the traces in (17) and in computation of the number density [see Eq. (4)] using the stochastic estimator method. $N_{\mathrm{stoch}} = 1000$ stochastic vectors are used to compute the traces in (17) in the deconfinement phase and 200 stochastic vectors in the confinement phase. For the number density computations we take $N_{\mathrm{stoch}} = 600$. We have checked that further increasing of N_{stoch} does not change our results.

IV. FITS OF THE NUMBER DENSITY TO EQS. (10) AND (11)

In Ref. [18] it was shown that the number density can be well described by a polynomial of θ in the deconfining phase (above T_{RW}) and by a few terms of the Fourier expansion below T_c. We will use this analysis and improve it in a few directions. First, we collected higher statistics and reduced the statistical errors substantially in comparison with Ref. [18]. Second, we simulate larger lattices: 16^3 in spatial directions instead of $16^2 \times 8$ in Ref. [18]. As a result we come to more solid statements about fitting.

In Fig. 2 we show results for n_{qI} as a function of θ for $T/T_c = 1.35, 1.20, 1.08$ for the range of θ values between 0.0 and $\pi/3$. n_{qI} is a continuous function over this range of θ. Results of the fits to function (10) are presented in Table I and also shown in the figure. For $T/T_c = 1.35$ we obtained a very good fit with $n_{\max} = 2$ with $\chi^2/N_{\mathrm{dof}} = 0.67$ for $N_{\mathrm{dof}} = 24$. An attempt to take $n_{\max} = 3$ and compute a_5 gave $a_5 = 0.008(20)$ with practically unchanged a_1 and a_3. Thus a_5 is not computable in this case. In opposite, at lower temperature $T/T_c = 1.20$ we needed fitting function with $n_{\max} = 3$. We obtained a good fit in this case.

The behavior of n_{qI} at $T/T_c = 1.08$ is different from that at higher temperatures discussed above. This temperature is below T_{RW} and at $\theta = \pi/3$ there is no first order phase transition, n_{qI} is continuous. Instead there is a crossover to the confinement phase at about $\theta = 0.92(2)$ as is indicated by the Polyakov loop susceptibility, see Fig. 3.

It is not yet clear how to fit the data over the range of μ_{qI} covering both the deconfining and the confining phase. Our data can be well fitted to various functions which give rise to very different behavior of the number density at real chemical potential. We need to increase our statistics

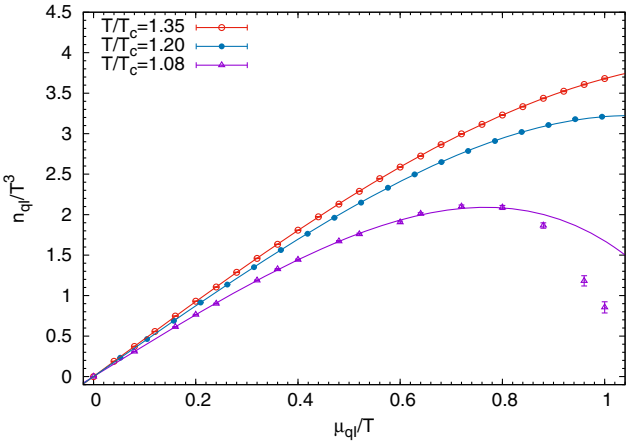

FIG. 2. Imaginary density as a function of θ in the deconfinement phase at temperatures $T/T_c = 1.35, 1.20, 1.08$. The curves show fits to function (10).

TABLE I. Results of fitting data for n_{qI}/T^3 in the deconfinement phase to function (10). Results for the Taylor coefficients c_2 and c_4 from Ref. [21] are shown for comparison with our results for a_1 and a_3, respectively.

T/T_c	a_1	a_3	a_5	$\chi^2/N_{\rm dof}, N_{\rm dof}$	$2c_2$	$-4c_4$
1.35(7)	4.671(2)	−0.991(4)	⋯	0.67, 24	4.682(11)	−0.97(8)
1.20(6)	4.409(6)	−1.032(31)	−0.165(32)	0.70, 16	4.403(14)	−1.30(15)
1.08(5)	3.880(17)	−1.62(21)	−0.59(0.47)	1.10, 9	3.877(19)	−1.33(17)

substantially to reduce the number of functions suitable for fitting of our data. For this reason in this work we made fit to function (10) over the range [0, 0.8], i.e. for deconfining phase. In this case we should consider the fit as a Taylor expansion. We needed again $n_{\rm max} = 3$ to obtain a good fit. Further increasing of $n_{\rm max}$ produced no reasonable results.

Now we can compare our results for constants a_i with the Taylor expansion results obtained in [21] (Table IV, lower part) for the same parameters of lattice QCD action as we used in our work. We find that there is an agreement between our values for $a_{1,3}$ and respective values obtained in [21] within error bars (note that relations between our constants $a_{1,3}$ and constants $c_{2,4}$ used in [21] are $c_2 = a_1/2, c_4 = -a_3/4$). It should be noted that for $T/T_c = 1.35$ and 1.20 where we produced many data points our error bars are substantially lower than error bars quoted in [21] (at $T/T_c = 1.08$ smaller error bars can be also achieved after increasing the number of data points). Furthermore, we were able to compute coefficient a_5 while in [21] corresponding coefficient c_6 was not computed due to complexity of the problem. This usefulness of simulations at the imaginary chemical potential to compute the Taylor expansion coefficients for pressure was suggested in [30–32]. This was recently confirmed in [19] where 2 + 1 lattice QCD with physical quark masses and in the continuum limit was studied. We confirm here their observations for a completely different set of parameters and different action of lattice QCD.

Next we compute Z_n using the procedure described in the previous section. Equation (8) now becomes

$$Z_n = \frac{\int_0^{2\pi} \frac{d\theta}{2\pi} \cos(n\theta) e^{-\frac{1}{N}\sum_m a_{2m-1}\theta^{2m}/(2m)}}{\int_0^{2\pi} \frac{d\theta}{2\pi} e^{-\frac{1}{N}\sum_m a_{2m-1}\theta^{2m}/(2m)}}. \quad (20)$$

We computed these integrals numerically using the multiprecision library [33]. It has been shown in [34] that there is a strong cancellation in the Fourier integral so using multiprecision in calculations is unavoidable. In fact we figured out that the number of precision digits needed depends on the phase because in different phases Z_n have different decreasing rates when n increases. In our calculations we used up to 1200 digits to be sure that results do not depend on precision. Results for Z_n are presented in Fig. 4 for n up to 300.

As a first check of the results for Z_n we computed n_{qI}/T^3 using Eq. (6) for $T/T_c = 1.35$ and 1.20. We found that the original data presented in Fig. 2 were reproduced nicely. The deviation for the full interval [0.0;1.0] was less than 0.6%.

As a more important check we compare our results for Z_n with Z_n obtained via hopping parameter expansion which was described in the previous section. The number of terms in Eq. (19) was taken equal to 60. Results obtained with the HPE method are also presented in Fig. 4. We use only 54 configurations to compute Z_n with HPE. For this reason the statistical error is much higher for this

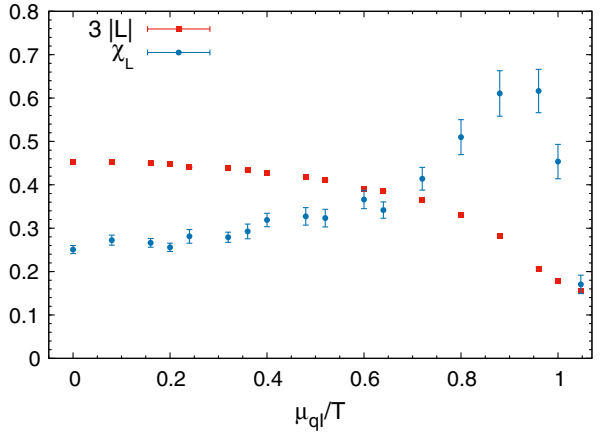

FIG. 3. The absolute value of the Polyakov loop (multiplied by factor 3) and its susceptibility vs μ_{qI} at $T/T_c = 1.08$.

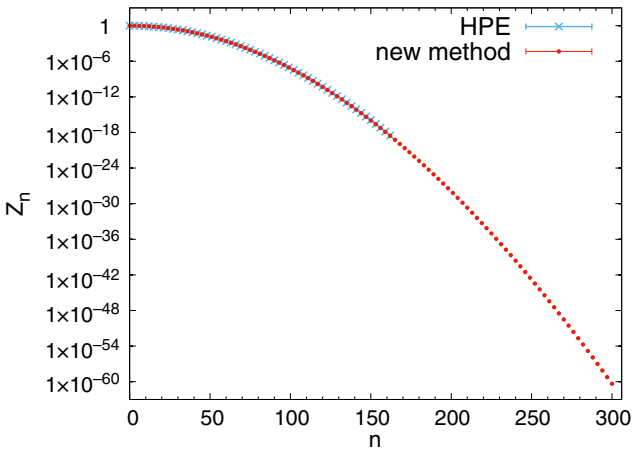

FIG. 4. Z_n vs n computed using two methods at $T/T_c = 1.35$.

method and we show only data up to $n = 162$ when relative statistical error reaches 50%.

One can see very nice agreement between two results although the values of Z_n change by almost 20 orders of magnitude. As a more careful check of this agreement we show in Fig. 5 the relative deviation of two results:

$$R = \frac{Z_{n,1} - Z_{n,2}}{Z_{n,1}}, \tag{21}$$

where $Z_{n,i}, i = 1, 2$ are for the new method and HPE, respectively. One can see that the relative deviation is compatible with zero for all presented values of n. Large statistical errors for large values of n come from the HPE result and can be reduced when full available statistics is used.

Although both methods we use to compute Z_n are approximate their systematic errors are of different nature. Thus agreement of results is not a coincidence. The fact that we obtained correct values for Z_n implies that the fit (10) with $n_{\max} = 2$ is not just a Taylor expansion valid for small values of the chemical potential only but rather a good approximation valid also for large values of the chemical potential. The range of validity depends on the range of values of index n for which the agreement between two methods extends. This statement should be further checked by computation of Z_n via the HPE method for higher n as well as for other temperatures in the deconfinement phase.

We fitted Z_n to function $e^{P(n)}$ where $P(n)$ is a polynomial function,

$$P(n) = p_2 n^2 + p_4 n^4 + p_6 n^6. \tag{22}$$

We found that this function fits the data extremely well: $\chi^2/N_{dof} = 0.028$ for $N_{\rm dof} = 97$. Small $\chi^2/N_{\rm dof}$ might indicate overestimated statistical errors or strong correlations between Z_n. Parameter values obtained are as follows:

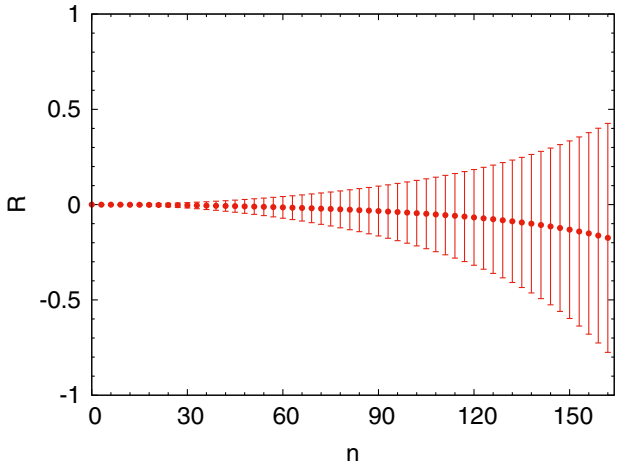

FIG. 5. Relative deviation of results for Z_n obtained by new and HPE methods vs n at $T/T_c = 1.35$.

$p_2 = -0.00167592(6)$, $p_4 = 1.909(4) \times 10^{-9}$, $p_6 = -5.08(6) \times 10^{-15}$. The relative deviation of the fitting function from the data is less than 0.08%. When the fit is made over the range $n \in [0, 100]$ then the prediction for $100 < n < 300$ has a relative deviation from the true result less than 1.5%. This illustrates the usefulness of the fitting of the data for Z_n in the deconfinement phase to function $e^{P(n)}$ when the data are known only for the restricted range of index n values. One can make extrapolation to much higher values of n with a rather small error of extrapolation.

Next we come to the confining phase results. In Fig. 6 we show n_{ql} for $\theta \in [0, \pi/3]$ together with fits to Eq. (11). The fit results are presented in Table II. We found good fits with $n_{\max} = 1$ for $T/T_c = 0.84$, 0.93 while for $T/T_c = 0.99$ fit with $n_{\max} = 2$ is necessary.

In Table II we also show coefficients a_1, a_3 and a_5 of the Taylor expansion of Eq. (11) as well as respective results from [21]. We see again agreement within error bars with Ref. [21] for the first two Taylor expansion coefficients and substantially smaller error bars in our work than in [21]. The third coefficient was not computed in [21]. We shall note that dependence of our third Taylor coefficient a_5 on the temperature is in qualitative agreement with results of Refs. [19,35] where $N_f = 2 + 1$ lattice QCD was studied. In both papers this coefficient (c_6 in notations of [19,35], $c_6 = a_5/6$) was found positive slightly below T_c, negative slightly above T_c and zero otherwise.

Equation (8) to compute Z_n now looks as follows:

$$Z_{3n} = \frac{\int_0^{2\pi} \frac{d\theta}{2\pi} \cos(3n\theta) e^{\sum_{m=1}^{n_{\max}} \tilde{f}_{3m} \cos(3m\theta)}}{\int_0^{2\pi} \frac{d\theta}{2\pi} e^{\sum_{m=1}^{n_{\max}} \tilde{f}_{3m} \cos(3m\theta)}} \tag{23}$$

$$= \frac{\int_0^{6\pi} \frac{dx}{6\pi} \cos(nx) e^{\sum_{m=1}^{n_{\max}} \tilde{f}_{3m} \cos(mx)}}{\int_0^{6\pi} \frac{dx}{6\pi} e^{\sum_{m=1}^{n_{\max}} \tilde{f}_{3m} \cos(mx)}}, \tag{24}$$

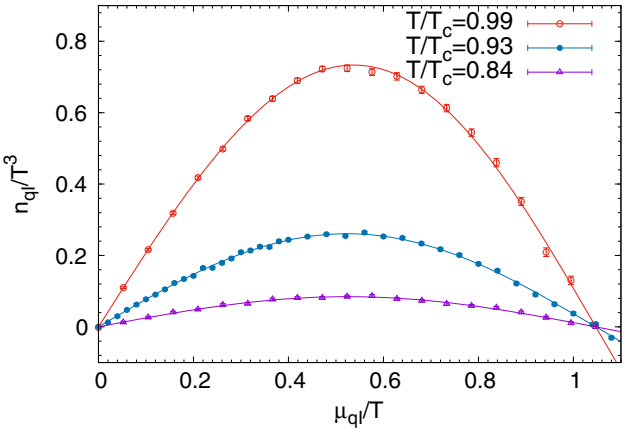

FIG. 6. Imaginary density as a function of θ at three temperatures in the confining phase. The curves show fits to function (11) with $n_{\max} = 1$ for $T/T_c = 0.84$, 0.93 and $n_{\max} = 2$ for $T/T_c = 0.99$.

TABLE II. Results of fitting data for n_{qI}/T^3 in the confinement phase to function (11) together with respective Taylor coefficients a_1, a_3, a_5. Results for the Taylor coefficients c_2 and c_4 from Ref. [21] are shown for comparison with our results for a_1 and a_3, respectively.

T/T_c	f_3	f_6	a_1	a_3	a_5	$\chi^2/N_{\rm dof}, N_{\rm dof}$	$2c_2$	$-4c_4$
0.99	0.7326(25)	−0.0159(21)	2.102(5)	−2.719(17)	0.453(55)	0.83, 18	2.071(34)	−2.9(8)
0.93	0.2608(8)	⋯	0.7824(24)	−1.1736(36)	0.5281(16)	0.93, 37	0.713(40)	−0.3(8)
0.84	0.0844(7)	⋯	0.2532(21)	−0.3798(31)	0.1709(14)	0.41, 18	0.251(35)	−0.0(6)

where $\tilde{f}_{3n} = \frac{N_s^3}{N_t^3}\frac{f_3}{3n}$. In case $n_{\max} = 1$ this can be expressed as

$$Z_{3n} = \frac{I_n(\tilde{f}_3)}{I_0(\tilde{f}_3)}, \tag{25}$$

where $I_n(x)$ is the modified Bessel function of the first kind. Results for Z_n at $T/T_c = 0.93$ are presented in Fig. 7.

Again, we first check if computed Z_n reproduce data for n_{qI}/T^3 and find nice agreement between data and values of n_{qI}/T^3 computed via Eq. (6). The deviation for the full interval $[0.0; \pi/3]$ was less than 0.3%.

Next we compare with hopping parameter expansion, respective results are also presented in Fig. 7. We used full statistics (1800 configurations at $\mu_{qI} = 0$) and W_n up to $n = 15$ in Eq. (18) for this computation. One can see agreement between two results up to $n = 21$. We believe that the disagreement for higher n is explained by inaccuracy in computation of Z_n computed by HPE. The statistical errors for Z_n grow very fast with n. It is necessary to improve the HPE method accuracy before the conclusion about agreement at large n can be made.

Still our result indicates that at $T/T_c = 0.93$ the fit function (11) provides correct values of Z_n and thus its analytical continuation should be valid up to values of μ_q/T beyond Taylor expansion validity range. Precise determination of the range of validity of this analytical continuation will be made in the future after getting more precise results for the HPE method. In Fig. 8 we show results for Z_n for all three temperatures below T_c. We stop to show data in this figure when the relative statistical error reaches 100%.

Let us note that one can derive a recursion relation for Z_n when n_{qI} is presented by function (11) with finite $n_{\max}$. For derivation see Appendix A. In particular for $n_{\max} = 1$ the recursion is just a recursion for I_n which is of the form

$$\tilde{f}_3(Z_{3(n-1)} - Z_{3(n+1)}) = 2nZ_{3n}. \tag{26}$$

Also one can get asymptotics for Z_n at large n. For $n_{\max} = 1$ it is

$$Z_{3n} = B\frac{(\tilde{f}_3/2)^n}{n!}, \tag{27}$$

where B is some constant. This asymptotics is shown in Fig. 8 for $T/T_c = 0.84$ and 0.93 with constant B obtained by fitting over the range $400 < n < 600$: $B = 0.02813((1)$ for $T/T_c = 0.93$ and $B = 0.219(2)$ for $T/T_c = 0.84$.

For $n_{\max} = N$ it is different:

$$Z_{3n} = B\frac{(\tilde{f}_{3N})^{n/N}}{\Gamma(n/N+1)}, \tag{28}$$

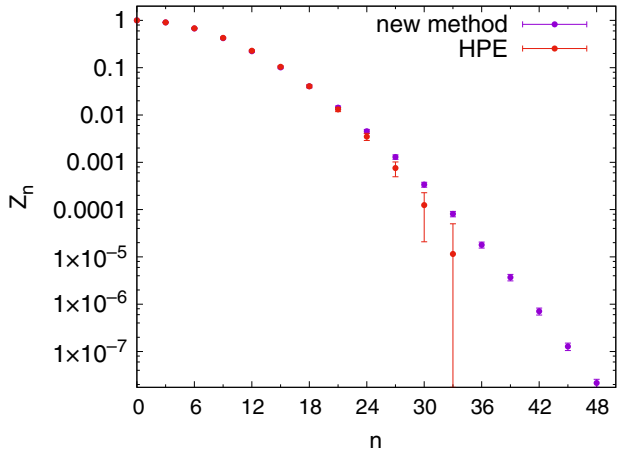

FIG. 7. Z_n vs n computed using two methods at $T/T_c = 0.93$.

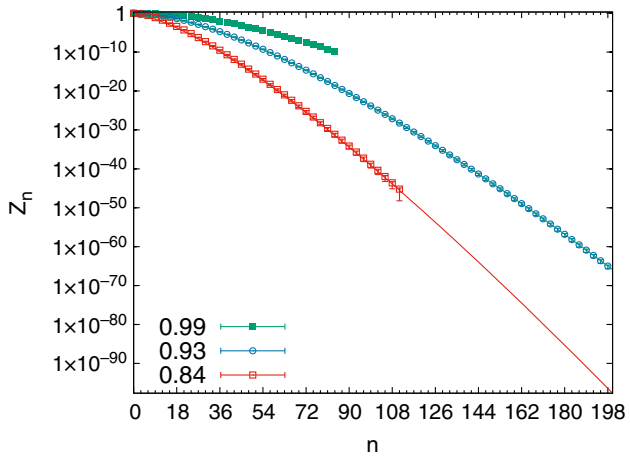

FIG. 8. Z_n vs n for three temperatures in the confinement phase. The curves show results of fitting to asymptotic behavior for $T/T_c = 0.93$ and 0.84.

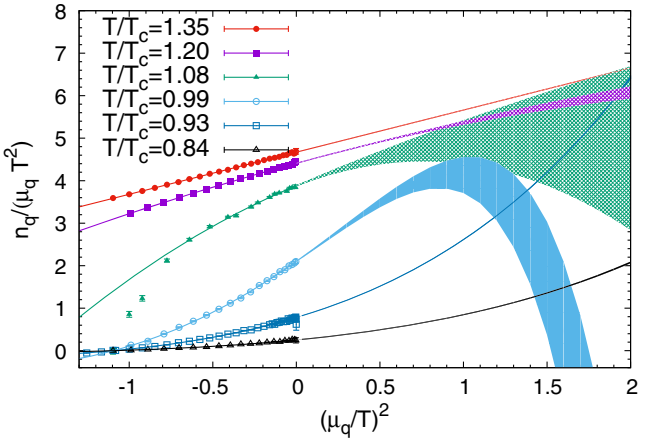

FIG. 9. Analytical continuation for the number density vs μ_q^2 for all temperature values. The curves show respective fits. The width of the curves shows the statistical error of extrapolation to $\mu_q^2 > 0$.

see Appendix A for derivation. From this asymptotics it follows in particular that the coefficient f_{3N} has to be positive, otherwise the condition of positivity of Z_{3n} will not hold. Our current fitting function for $T/T_c = 0.99$ which has $f_{3N} \equiv f_6 < 0$ does not satisfy this requirement. We need to improve statistics for this temperature to obtain the coefficient for the next harmonics in Eq. (11). Evidently with the present fitting function we cannot go to large values of μ_q for this temperature.

At the end of this section we show in Fig. 9 ratio $\frac{n_q}{\mu_q T^2}$ as a function of μ_q^2 for negative and positive values. The analytical continuation to positive μ_q^2 values was made in Eqs. (10) and (11) by the change of θ to $i\theta$. The range of validity of this analytical continuation is discussed in the Sec. V. This way of presentation, borrowed from [19], allows one to show in one plot the simulation results obtained at $\mu_q^2 < 0$ and analytical continuation of our fitting functions to $\mu_q^2 > 0$. One can see that analytical continuation has reasonable statistical errors up to large values of $(\mu_q/T)^2$ for the two highest temperatures and the two lowest temperatures. For temperatures $T/T_c = 0.99$, 1.08 we need to improve statistics.

Let us note that another possibility to check the range of validity of the new method suggested in this paper is to make simulations in a model without the sign problem like QC_2D [36,37]. We are planning to do such checks in the future.

V. CONCLUSIONS

We have presented a new method to compute the canonical partition functions Z_n. It is based on fitting of the imaginary number density for all values of imaginary chemical potential to the theoretically motivated fitting functions: polynomial fit (10) in the deconfinement phase for T above $T_{\rm RW}$ and Fourier-type fit (11) in the confinement phase. The proper fit for temperatures between T_c and $T_{\rm RW}$ has not been found in this work and is a subject of future study. For this temperature range we used the polynomial fit for the restricted range of μ_{qI}.

Using fit results we compute the canonical partition functions $Z_n \equiv \frac{Z_C(n,T,V)}{Z_C(0,T,V)}$ at five values of T/T_c (all temperatures apart from $T/T_c = 1.08$) via Fourier transformation (8). It was necessary to use the multiprecision library [33] to compute Z_n which change over many orders of magnitude. For all temperatures we have checked that precision of computation of Z_n was high enough to reproduce the imaginary number density n_{qI} via Eq. (6).

At temperatures $T/T_c = 1.35$ and 0.93 we compared our results for Z_n with Z_n computed by hopping parameter expansion. We found that the new method works in both confinement and deconfinement phases: two sets of Z_n computed by completely independent methods agree well, see Figs. 4 and 7. This means that the fitting functions used in this work are proper approximations for the imaginary number density in the full range of μ_{qI} values. Furthermore, this means that the analytical continuation to the real chemical potential can in principle be done beyond the Taylor expansion validity range since this analytical continuation coincides with n_q computed with the help of correctly determined Z_n via Eq. (5). Thus the new method allows one to compute the number density n_q beyond Taylor expansion. The range of validity of the new method including the analytical continuation presented in Fig. 9 is implicitly determined by the number of correctly computed Z_n. This number can be increased by increasing the quality of approximation of imaginary number density. This can be achieved when more terms in Eqs. (10) and (11) are determined via the fitting procedure or via direct numerical computation of the integral (7).

The agreement of the new method and the HPE method is especially remarkable in the deconfining phase, see Figs. 4 and 5. The deconfinement region is being explored extensively by ALICE experiments at LHC [2]. Note that our new method is not limited to the heavy quark mass values like HPE, nor small μ values like Taylor expansion. Once we calculate Z_n using the new method, we can calculate any thermodynamical quantities, pressure, number density and its higher moments. Thus the new method can provide very reliable theoretical basis for LHC results. We plan to calculate these quantities with much smaller quark mass in order to give first-principle theoretical results for comparison with LHC data.

We believe that the new method will also help to determine the transition line in the temperature-chemical potential plane. Respective results will be presented in a forthcoming publication after data with higher statistics will be accumulated and results for lower quark masses will be obtained.

Using our results for the number density n_{qI} we computed the Taylor expansion coefficients for the number density from which respective coefficients for the pressure are easily restored. We found good agreement with earlier results obtained in [21] via direct computation of these coefficients. Moreover, we found that our error bars for these coefficients are in general substantially smaller than error bars quoted in [21]. Thus we confirmed analogous observation made in [19]. Our estimation for sixth order Taylor coefficients c_6 which were not computed in [21] are in good qualitative agreement with results of Refs. [19,35].

We found that obtained at $T/T_c = 1.35$ Z_n values are nicely described by the exponential behavior with polynomial (22) in the exponent. We checked that this fit works over the range of n up to 300 which corresponds to quark density $n_q/T^3 \approx 5$. For $T < T_c$ we obtained asymptotics of Z_n at large n which indicates slower decreasing of Z_n with n than in the deconfining phase, see Eq. (28). Still this decreasing is fast enough to provide convergence of the infinite sums in Eqs. (2) and (5).

ACKNOWLEDGMENTS

The authors are grateful to Ph. de Forcrand and M. Hanada for useful discussions. This work was completed due to support by the Russian Science Foundation Grant under Contract No. 15-12-20008. Computer simulations were performed on the FEFU GPU cluster Vostok-1 and MSU "Lomonosov" supercomputer.

APPENDIX: RECURSION RELATIONS FOR Z_{3n}

In this Appendix we derive a recursion relation for Z_{3n} in the confinement phase. Let us introduce notations $3\theta = x$, $\tilde{f}_n = f_n/(2C)$.

For the case of $n_{\max} > 1$ in Eq. (11) it is possible to derive a recursion relation similar to relation (26). Let us show this for $n_{\max} = 2$. We have

$$\tilde{f}_3 \sin(x) + \tilde{f}_6 \sin(2x) = \frac{\sum_n n Z_{3n} \sin(nx)}{1 + 2\sum_n Z_{3n} \cos(nx)}. \quad \text{(A1)}$$

Then

$$(\tilde{f}_3 \sin(x) + \tilde{f}_6 \sin(2x))\left(1 + 2\sum_n Z_{3n} \cos(nx)\right) = \sum_n n Z_{3n} \sin(nx).$$

Computing Fourier modes on both sides we get

$$\tilde{f}_3 \int_{-\pi}^{\pi} dx \sin(x)\left(1 + 2\sum_n Z_{3n} \cos(nx)\right) \sin(mx) + \tilde{f}_6 \int_{-\pi}^{\pi} dx \sin(2x)\left(1 + 2\sum_n Z_{3n} \cos(nx)\right) \sin(mx) = \int_{-\pi}^{\pi} dx \sum_n n Z_{3n} \sin(nx) \sin(mx) \quad \text{(A2)}$$

$$\tilde{f}_3 (Z_{3(m-1)} - Z_{3(m+1)}) + \tilde{f}_6 (Z_{3(m-2)} - Z_{3(m+2)}) = m Z_{3m} \quad \text{(A3)}$$

or

$$Z_{3(m+2)} = Z_{3(m-2)} - \frac{m}{\tilde{f}_6} Z_{3m} + \frac{\tilde{f}_3}{\tilde{f}_6}(Z_{3(m-1)} - Z_{3(m+1)}). \quad \text{(A4)}$$

We need f_3, f_6, Z_3, Z_6 to compute all $Z_{3m}, m > 2$.

The asymptotical behavior in this case is

$$Z_{3n} = B \frac{(\tilde{f}_6)^{n/2}}{\Gamma(n/2 + 1)}. \quad \text{(A5)}$$

It is easy to get the recursion relation and asymptotics for $n_{\max} = N$. The recursion relation is

$$Z_{3(n+N)} = Z_{3(n-N)} - \frac{n}{\tilde{f}_{3N}} Z_{3n} + \sum_{m=1}^{N-1} \frac{\tilde{f}_{3(n-m)}}{\tilde{f}_{3N}} (Z_{3(n-m)} - Z_{3(n+m)}) \quad \text{(A6)}$$

and the asymptotics

$$Z_{3n} = B \frac{(\tilde{f}_{3N})^{n/N}}{\Gamma(n/N + 1)}. \quad \text{(A7)}$$

Some conclusions might be drawn from this expression. The asymptotics is determined by the highest mode. Thus f_{3N} has to be positive. Decreasing of Z_n becomes weaker with increasing N.

The numerical data for $n_{qI}(\theta)$ indicate that in the confinement phase the number of modes N necessary to describe the data is finite. Then the above considerations apply. We can make a statement that the radius of convergence is infinite. In the deconfinement phase at temperatures $T > T_{\mathrm{RW}}$ where first order Roberge-Weiss transition takes place N is definitely infinite. In the range of temperature $T_c < T < T_{\mathrm{RW}}$ the situation is unclear.

[1] J. Adams *et al.* (STAR Collaboration), Nucl. Phys. **A757**, 102 (2005).
[2] K. Aamodt *et al.* (ALICE Collaboration), J. Instrum. **3**, S08002 (2008).
[3] S. Muroya, A. Nakamura, C. Nonaka, and T. Takaishi, Prog. Theor. Phys. **110**, 615 (2003).
[4] O. Philipsen, *Proc. Sci.*, LAT2005 (2006) 016 [arXiv:hep-lat/0510077].
[5] P. de Forcrand, *Proc. Sci.*, LAT2009 (2009) 010 [arXiv:1005.0539].
[6] K. Nagata and A. Nakamura, J. High Energy Phys. 04 (2012) 092.
[7] P. de Forcrand and S. Kratochvila, Nucl. Phys. B, Proc. Suppl. **153**, 62 (2006).
[8] S. Ejiri, Phys. Rev. D **78**, 074507 (2008).
[9] A. Li, A. Alexandru, K.-F. Liu, and X. Meng, Phys. Rev. D **82**, 054502 (2010).
[10] A. Li, A. Alexandru, and K.-F. Liu, Phys. Rev. D **84**, 071503 (2011).
[11] J. Danzer and C. Gattringer, Phys. Rev. D **86**, 014502 (2012).
[12] C. Gattringer and H.-P. Schadler, Phys. Rev. D **91**, 074511 (2015).
[13] R. Fukuda, A. Nakamura, and S. Oka, Phys. Rev. D **93**, 094508 (2016).
[14] A. Nakamura, S. Oka, and Y. Taniguchi, J. High Energy Phys. 02 (2016) 054.
[15] A. Hasenfratz and D. Toussaint, Nucl. Phys. **B371**, 539 (1992).
[16] A. Roberge and N. Weiss, Nucl. Phys. **B275**, 734 (1986).
[17] C. Bonati, P. de Forcrand, M. D'Elia, O. Philipsen, and F. Sanfilippo, Phys. Rev. D **90**, 074030 (2014).
[18] J. Takahashi, H. Kouno, and M. Yahiro, Phys. Rev. D **91**, 014501 (2015).
[19] J. Gunther, R. Bellwied, S. Borsanyi, Z. Fodor, S. D. Katz, A. Pasztor, and C. Ratti, EPJ Web Conf. **137**, 07008 (2017).
[20] F. Karsch, K. Redlich, and A. Tawfik, Phys. Lett. B **571**, 67 (2003).
[21] S. Ejiri, Y. Maezawa, N. Ukita, S. Aoki, T. Hatsuda, N. Ishii, K. Kanaya, and T. Umeda (WHOT-QCD Collaboration), Phys. Rev. D **82**, 014508 (2010).
[22] A. Hasenfratz and P. Hasenfratz, Phys. Lett. B **104**, 489 (1981).
[23] I. O. Stamatescu, Phys. Rev. D **25**, 1130 (1982).
[24] I. Bender, T. Hashimoto, F. Karsch, V. Linke, A. Nakamura, M. Plewnia, I. O. Stamatescu, and W. Wetzel, Nucl. Phys. B, Proc. Suppl. **26**, 323 (1992).
[25] R. De Pietri, A. Feo, E. Seiler, and I.-O. Stamatescu, Phys. Rev. D **76**, 114501 (2007).
[26] G. Aarts and I.-O. Stamatescu, J. High Energy Phys. 09 (2008) 018.
[27] G. Aarts, E. Seiler, D. Sexty, and I.-O. Stamatescu, Phys. Rev. D **90**, 114505 (2014).
[28] K. Nagata and A. Nakamura, Phys. Rev. D **82**, 094027 (2010).
[29] V. A. Goy, V. Bornyakov, D. Boyda, A. Molochkov, A. Nakamura, A. Nikolaev, and V. Zakharov, Prog. Theor. Exp. Phys. **2017**, 031D01 (2017).
[30] M. D'Elia and F. Sanfilippo, Phys. Rev. D **80**, 014502 (2009).
[31] T. Takaishi, P. de Forcrand, and A. Nakamura, *Proc. Sci.*, LAT2009 (2009) 198 [arXiv:1002.0890].
[32] E. Laermann, F. Meyer, and M. P. Lombardo, J. Phys. Conf. Ser. **432**, 012016 (2013).
[33] D. M. Smith, http://myweb.lmu.edu/dmsmith/fmlib.html.
[34] S. Oka (LATTICE-Zn Collaboration), *Proc. Sci.*, LATTICE2015 (2016) 166 [arXiv:1511.04711].
[35] C. R. Allton, M. Doring, S. Ejiri, S. J. Hands, O. Kaczmarek, F. Karsch, E. Laermann, and K. Redlich, Phys. Rev. D **71**, 054508 (2005).
[36] T. Makiyama, Y. Sakai, T. Saito, M. Ishii, J. Takahashi, K. Kashiwa, H. Kouno, A. Nakamura, and M. Yahiro, Phys. Rev. D **93**, 014505 (2016).
[37] V. V. Braguta, E. M. Ilgenfritz, A. Yu. Kotov, A. V. Molochkov, and A. A. Nikolaev, Phys. Rev. D **94**, 114510 (2016).